ARTICLES

Journal of Semiconductors
(2022) 43, 022801
doi: 10.1088/1674-4926/43/2/022801

Structural and optical properties of AlN sputtering deposited on sapphire substrates with various orientations

Xianchun Peng[1, 2, ‡], Jie Sun[1, ‡], Huan Liu[3, 4], Liang Li[1], Qikun Wang[4], Liang Wu[4], Wei Guo[1, †], Fanping Meng[1, †], Li Chen[1], Feng Huang[1], and Jichun Ye[1, †]

[1]Ningbo Institute of Materials Technology and Engineering, Chinese Academy of Sciences, Ningbo 315201, China

[2]Faculty of Materials Science and Chemical Engineering, Ningbo University, Ningbo 315211, China

[3]State Key Laboratory of Advanced Special Steel, Shanghai Key Laboratory of Advanced Ferrous Metallurgy, School of Materials Science and Engineering, Shanghai University, Shanghai 200044, China

[4]Ultratrend Technologies Inc., Hangzhou 311199, China

Abstract: AlN thin films were deposited on *c*-, *a*- and *r*-plane sapphire substrates by the magnetron sputtering technique. The influence of high-temperature thermal annealing (HTTA) on the structural, optical properties as well as surface stoichiometry were comprehensively investigated. The significant narrowing of the (0002) diffraction peak to as low as 68 arcsec of AlN after HTTA implies a reduction of tilt component inside the AlN thin films, and consequently much-reduced dislocation densities. This is also supported by the appearance of E_2(high) Raman peak and better Al–N stoichiometry after HTTA. Furthermore, the increased absorption edge after HTTA suggests a reduction of point defects acting as the absorption centers. It is concluded that HTTA is a universal post-treatment technique in improving the crystalline quality of sputtered AlN regardless of sapphire orientation.

Key words: nitrides; physical vapor deposition processes; semiconducting III–V materials; defects

Citation: X C Peng, J Sun, H Liu, L Li, Q K Wang, L Wu, W Guo, F P Meng, L Chen, F Huang, and J C Ye, Structural and optical properties of AlN sputtering deposited on sapphire substrates with various orientations[J]. *J. Semicond.*, 2022, 43(2), 022801. http://doi.org/10.1088/1674-4926/43/2/022801

1. Introduction

AlN thin film is a material of great technological advantage due to its ultrawide bandgap, high breakdown voltage and strong spontaneous polarization field. Serving as a template, a variety of optoelectronic, power and RF devices are grown on top of it, including the ultraviolet light-emitting-diode (UV-LED), laser diodes and Schottky barrier diode[1–6]. Pheudomorphic AlGaN thin films with compressive strains were successfully grown on top of the AlN with well controlled crystalline quality, leading to efficient carrier recombination or large breakdown voltage[7–10]. Additionally, AlN thin film was also identified as a potential candidate in the development of high-temperature surface or bulk acoustic filters due to its high temperature stability, excellent propagation velocity and good piezoelectric properties[11].

Due to the lack of bulk AlN substrate with suitable size and satisfied crystalline quality, intensive efforts were paid to heteroepitaxy growth of AlN on foreign substrates including sapphire, SiC, and Si. As a result, the challenges of lattice and thermal mismatch during epitaxial growth must be taken care of. Among various epitaxial growth techniques, metal organic chemical vapor deposition (MOCVD) has been regarded as one of the most mature technologies in AlN deposition. However, epitaxial growth of AlN by MOCVD has relatively low production yield, considering the lack of a high-volume, high-temperature growth chamber. Compared with MOCVD, sputtering is an alternative technique to achieve uniform AlN thin film with size up to 6 inches at a relatively low cost[12, 13]. This technique is suitable for fabrication scale-up in view of the low equipment cost and absence of growth by-products[14]. Nevertheless, AlN films prepared by sputtering usually suffer from poor quality due to lacking of energy for adatom diffusion under low deposition temperature. This leads to columnar growth nature of the AlN with increasing number of threading dislocations and point defects, which greatly deteriorating the performance of the semiconductor devices.

Recently, high-temperature thermal annealing (HTTA) above 1500 °C has been acknowledged as an effective way to improve the crystallinity of AlN[15–17]. The thermal annealing on sputtered AlN was firstly reported by Miyake in 2016 utilizing a "face-to-face" annealing configuration. A low threading dislocation density (TDD) of 4.7×10^8 cm^{-2} was reported, comparable to the value of AlN on a sapphire substrate by the MOCVD technique[13]. The improved crystalline quality was ascribed to the coalescence of columnar domains at elevated temperature[18]. As a result, AlN thin films achieved by sputtering followed by post-growth HTTA are considered to be potential candidates in the realization of high performance optoelectronic/electronic devices[13, 19].

Nevertheless, despite many promising results reported on sputtered AlN thin films with HTTA, there is still a lack of comprehensive investigations on the influence of HTTA on op-

Xianchun Peng and Jie Sun contributed equally to this work.
Correspondence to: W Guo, guowei@nimte.ac.cn; F P Meng, mengfp@nimte.ac.cn; J C Ye, jichun.ye@nimte.ac.cn
Received 6 JULY 2021; Revised 25 AUGUST 2021.

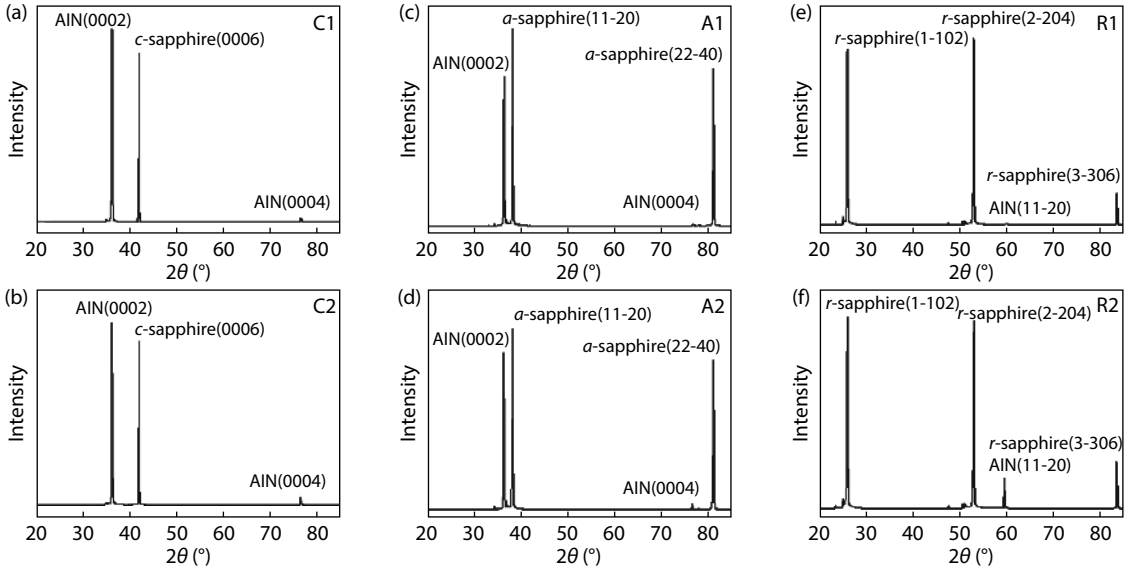

Fig. 1. Powder X-ray diffraction spectra of AlN deposited on (a, b) *c* , (c, d) *a* and (e, f) *r*-plane sapphire substrates before and after thermal annealing. Clear diffraction peaks from AlN and sapphire can be identified.

tical properties, surface stoichiometry and strain behaviors of the sputtered AlN thin films. In addition, it is well known that sputtered AlN thin films on *c*-plane sapphire substrate usually exhibit +*c* crystal orientation. Yet non-polar and semi-polar crystallographic planes are desired due to much-reduced polarization fields and consequently less influence from the quantum-confined Stark effect[20, 21]. As a result, in-depth exploration regards to the influence of sapphire orientation on the structural and optical properties of AlN is needed.

In this paper, AlN deposited on a sapphire substrate with different orientations (*c*, *a*, and *r* crystallographic planes) was achieved by the magnetron sputtering technique followed by HTTA. The correlations between the structural, optical, strain states as well as chemical stoichiometry of the HTTA AlN were provided. The scope of this work is to investigate the applicability of sputtered AlN grown on sapphire substrates with various orientations after HTTA, and offer design rules for the development large-size, high-performance AlN-based optoelectronic and electronic devices.

2. Experiment

AlN thin films were deposited on (0001) *c*-plane, non-polar (11-20) *a*-plane and semi-polar (10-12) *r*-plane 2-inch sapphire substrates via radio frequency (RF) magnetron sputtering technique. The deposition was performed in a custom-built MS450 sputter deposition system as previously reported[22, 23]. Prior to thin film deposition, sapphire substrates were degreased with acetone, methanol and deionized (DI) water in an ultrasonic bath and dried with nitrogen gas. The target thickness of the AlN thin film is approximately 300 nm. A high purity (99.999 at.%) of Al target of 100 mm in diameter was chosen as the Al source. Before AlN thin film deposition, the base pressure was pumped down to at least 5×10^{-5} Pa, followed by gradually heating up the substrates up to 580 °C. The deposition chamber was then filled with a mixture of nitrogen and argon gas at 35% N_2/65% Ar ratio with a total working pressure of 0.8 Pa. Sapphire substrates with various orientations were placed on the sample holder at the same time during thin film deposition. The substrate holder was rotated at a speed larger than 12 cycle/min, guaranteeing the uniform deposition of AlN. After AlN deposition, some of the wafers were put into the annealing chamber (Ultratrend Technologies Inc., Hangzhou, China) for post-deposition thermal treatment under N_2 atmosphere with temperature as high as 1700 °C. A face-to-face annealing was adopted in order to avoid thin film decomposition. For notation purposes, as deposited AlN thin films on *c*, *a* and *r*-oriented sapphire substrates are denoted as C1, A1, and R1, respectively, whereas corresponding AlN thin films subjected to thermal annealing are denoted as C2, A2, and R2.

The surface morphologies of the AlN thin film prior to and after HTTA were characterized by Veeco Dimension 3100V atomic force microscopy (AFM). The crystal orientation and thin film quality of AlN thin films were measured by both powder X-ray diffraction (XRD) and high-resolution X-ray diffraction (HRXRD) with an asymmetric Ge (220) monochromator. The thickness of the AlN film is measured by a J.A. Woollam M-200DI spectroscopic ellipsometer. The optical transmission spectrum of the AlN was measured by a Perkin Elmer Lambda 950 UV/Vis/NIR spectrometer equipped with an integrating sphere. Bi-axial strain conditions were characterized by a Renishaw inVia Raman spectroscopy under confocal mode. The spectrum resolution is 1 cm^{-1}, and 532 nm green laser was used as the excitation source. Surface stoichiometry was investigated by a Kratos Axis Ultra DLD-ray photoelectron spectrometer (XPS).

3. Results and discussions

Fig. 1 shows the symmetric ω–2θ powder XRD diffractions of the AlN thin films sputter deposited on the sapphire substrates of *c*, *a*, and *r*-orientations with and without thermal annealing. (0002) diffraction peaks can be clearly identified from the AlN sputtered on *c* and *a*-plane sapphire substrates, indicating the successful epitaxial growth of AlN thin film. This is consistent with previous reports that c-oriented AlN is most frequently observed during sputtering[24, 25]. In contrast, only a weak (11-20) diffraction peak is detected for AlN deposited on *r*-sapphire. The intensity of the (0002) diffrac-

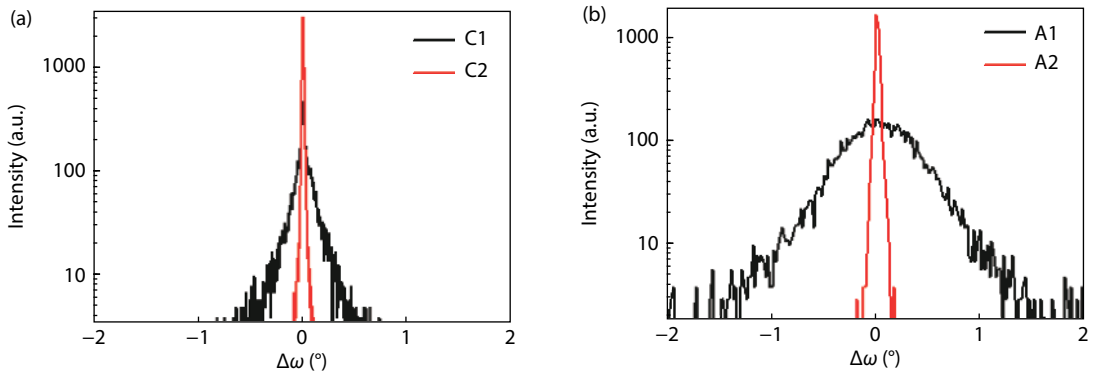

Fig. 2. (Color online) HRXRD (0002) RC scans of sputtered AlN on (a) *c*-plane and (b) *a*-plane sapphire substrates prior to and after thermal annealing.

tion peak for sample C1 is stronger than that of A1, which can be explained by the smaller lattice mismatch between the in-plane lattice constant of AlN and sapphire with 30° in-plane rotation. After HTTA, there is no obvious variation of the relative intensity of the (0002) peak of AlN deposited on *c* and *a*-plane sapphire, but there is a slight enhancement of AlN (11-20) peak for AlN deposited on ***r***-plane sapphire. This suggests that the influence of thermal annealing on crystalline quality of AlN is the most significant for non-polar AlN on *r*-plane sapphire.

To further validate the change in crystalline quality of AlN after HTTA, HRXRD rocking curve (RC) scans were employed. No significant (11-20) diffraction peak can be identified from the HRXRD scan of AlN deposited on *r*-sapphire possibly due to the inferior crystalline quality, thus only the results of C1/2 and A1/2 were illustrated in Fig. 2. Note that the full-width-half-maximum (FWHM) value of the (0002) RC diffraction peak is an indication of the density of screw-type dislocations, which is strongly correlated with the tilt component of the crystal grains[26]. For AlN deposited on *c*-plane sapphire substrate, FWHM of the AlN (0002) diffraction peak decreases from 252 arcsec to as low as 68 arcsec after thermal treatment, which is comparable to the best results of AlN epitaxially grown by MOCVD[27, 28]. For AlN grown on *a*-plane sapphire, the FWHM value also exhibits a drastic drop from 2494 to 151 arcsec. The significant narrowing of the FWHM of the (0002) peak of AlN translate into 14 times reduction of screw-type dislocations for AlN deposited on *c*-sapphire, and more than 274 times reduction of dislocations for AlN deposited on *a*-sapphire. The crystalline quality of AlN grown on *c*-plane and *a*-plane sapphire had been greatly improved after HTTA, in which case thermal annealing facilitates the coalescence of columnar domains of *c*-oriented AlN during sputtering and subsequent defect annihilation[18, 29]. However, asymmetric (10-12) diffraction peak of AlN deposited on *c* and *a*-sapphires cannot be identified, which can be ascribed to a large number of stacking faults, the existence of grain twist components and a reduced coherent length[30]. Comparing the HRXRD diffraction data of AlN deposited on *c,* and *a*-sapphire, it is demonstrated that due to a much better lattice match between AlN and *c*-sapphire, the epitaxial growth via sputtering followed by HTTA turns out to be a promising candidate in improving the crystalline quality of AlN.

Fig. 3 shows the AFM images of sputtered AlN deposited on *c, a* and *r*-plane sapphire substrates prior to and after thermal anneasling. Before HTTA, All AlN thin films exhibit columnar surface morphology, which can be ascribed to insufficient Al surface diffusivity at low deposition temperature. The root-mean-square (RMS) roughness are 1.66, 2.86 and 5.15 nm for C1, A1, and R1, respectively, indicating that better crystalline quality is usually associated with smaller surface roughness. Interestingly, all samples grow in columnar shape despite different crystallographic planes, suggesting that adatom nucleation and diffusion seem to dominate the sputtering process regardless of sapphire orientations. After HTTA, columns merged into each other, and the sizes of the crystal grains expanded. This is as expected since HTTA will promote the coalescence of small crystal grains, leading to annihilation of threading dislocations as previously mentioned. After HTTA, rms values of C2 and R2 increase to 2.03 and 6.11 nm respectively, consistent with the larger grain sizes. For AlN deposited on *a*-plane sapphire, i.e. A2, however, the surface roughness decreases to 0.717 nm, with most of the regions being atomically smooth. For samples of C2, R2, surface decomposition occurs at the very top surface, leading to large surface roughness. However, for sample A2, the dramatically coalescence of columnar domains of c-oriented AlN after HTTA is the main reason for the decrease of RMS roughness. Recall that in Fig. 2, the reduction of the FWHM of the (0002) diffraction peak of AlN on *a*-sapphire is the most dominant. Therefore, a strong correlation is herein established between the annihilation of dislocations and change in surface morphology. Nevertheless, due to a better matching of the crystal lattice between *c*-sapphire and *c*-AlN, AlN deposited on *c*-sapphire still exhibits the best crystalline quality of only 68 arcsec. While its surface morphology still remains grainy. The discrepancy could be explained by the different annihilation behaviors of dislocations between the surface and the bulk. Finally, it is worth noting that Uedono *et al.* have previously observed bi-layer steps on the AlN surface after thermal annealing, but unfortunately, this step-flow morphology was not observed in our case. The discrepancy can be attributed to the different annealing pressures and atmospheres in the experiment, which play critical roles in keeping the balance between dislocation annihilation and surface decomposition[31, 32].

AlN has a theoretical bandgap of 6.2 eV, but mid-gap light absorption strongly deteriorates its capability as a UV-transparent substrate in applications such as UV-LED and laser diode. It has been reported that point defects such as car-

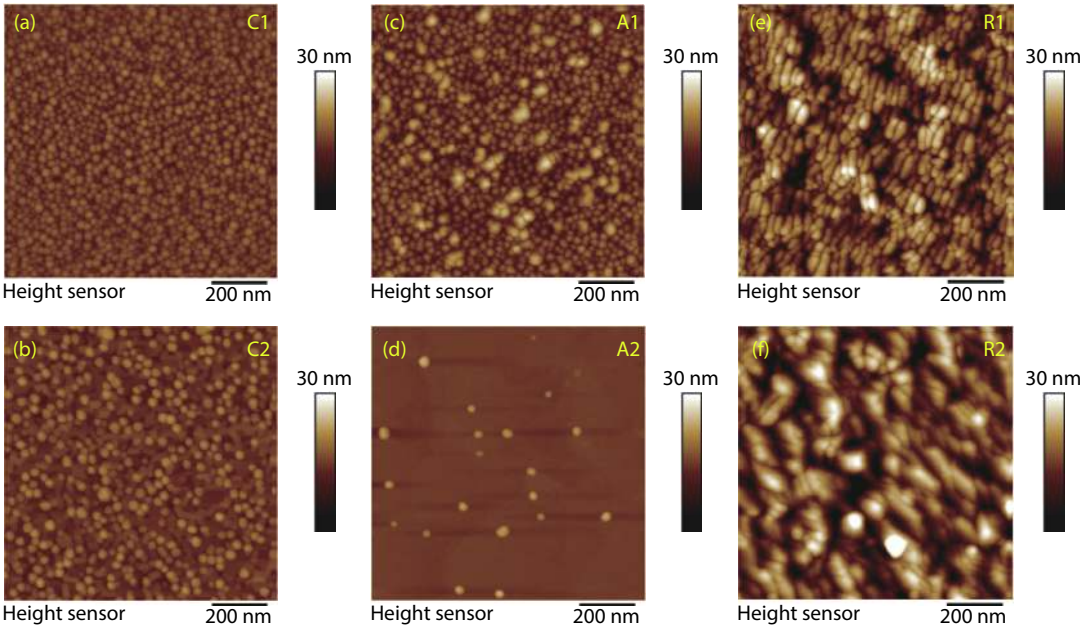

Fig. 3. (Color online) Surface morphology of sputtered AlN on (a, b) *c*, (c, d) *a*, (e, f) *r*-plane sapphires prior to (a, c, e) and after (b, d, f) thermal annealing.

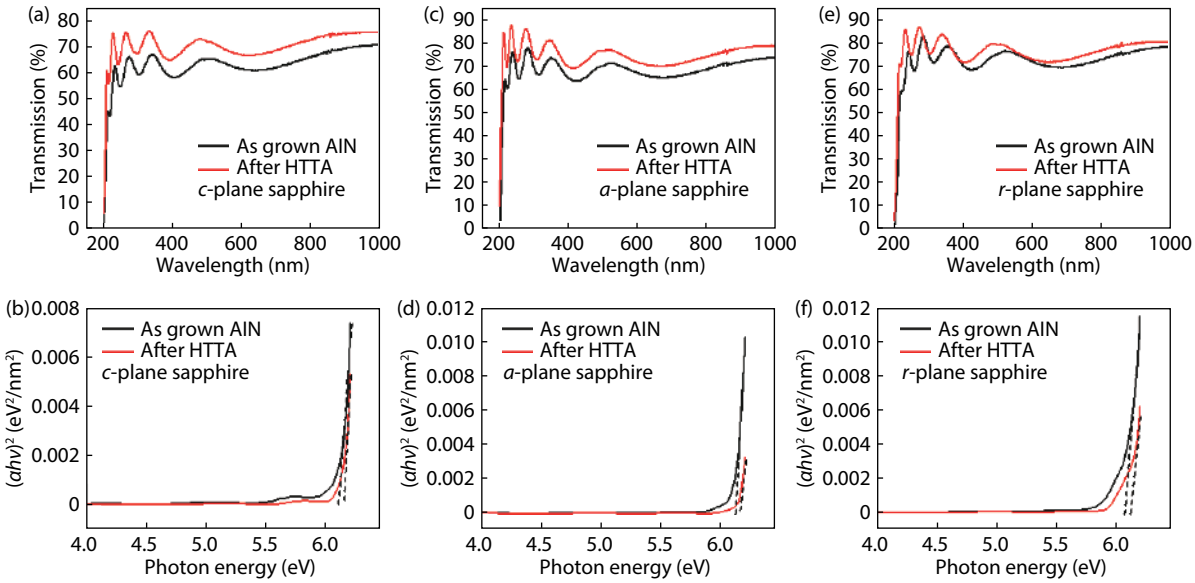

Fig. 4. (Color online) Optical transmission spectra and the square of absorption coefficient (α^2) versus photon energy ($h\nu$) of sputtered AlN on (a, b) *c*, (c, d) *a*, and (e, f) *r*-sapphire substrates before and after thermal annealing. The band gap is derived from the intersection between the linear fitting of the absorption curve and the *x* axis.

bon interstitials or vacancies can lead to strong UV absorption, making point defect control even more critical than that of dislocation[33]. To further investigate the influence of thermal annealing on the change in point defect and consequently optical properties of AlN, transmission curves were collected and illustrated in Figs. 4(a), 4(c), and 4(e). Dramatically enhanced light transmission was observed for all samples after thermal annealing. Note that the thickness fringes represent light reflections at the upper and lower interface of the AlN thin films. The thicknesses of AlN films can be calculated by Eq. (1). M is the number of interference fringes between two maximums or minimums ($M = 1$ means two adjacent maximums or minimums), n and λ are the corresponding refractive indexes and wavelengths. All samples exhibit a 10–20 nm thickness reduction possibly due to surface decomposition after HTTA. The relationship between the absorption coefficient (α), incident photon energy ($h\nu$), and the bandgap of AlN thin film (E_g) can be expressed in Eq. (2), where C is a constant[34]:

$$d = \frac{M\lambda_1\lambda_2}{2(n_{\lambda_1}\lambda_2 - n_{\lambda_2}\lambda_1)}, \tag{1}$$

$$\alpha h\nu = C\sqrt{h\nu - E_g}. \tag{2}$$

The bandgap of AlN thin films can be estimated by extrapolating the linear portion of the absorption coefficient curve to the x-axis as illustrated in Figs. 4(b), 4(d), and 4(f). The bandgap values as well as rms roughness and the FWHM of

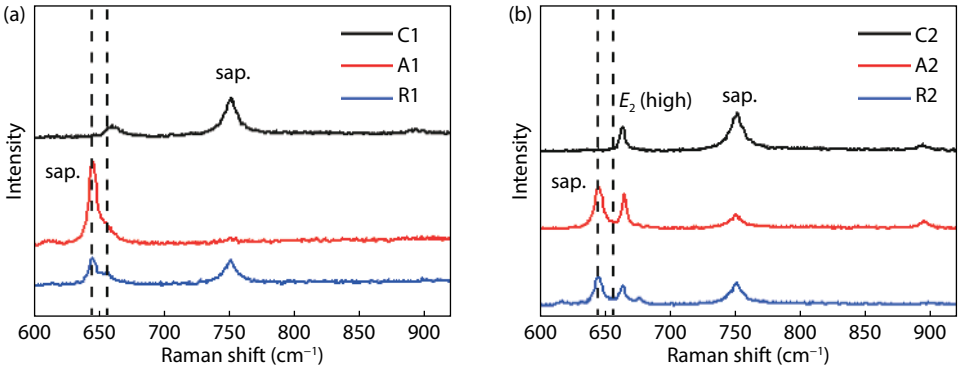

Fig. 5. (Color online) Raman spectra of sputtered AlN on *c*, *a*, and *r*-sapphire substrates (a) prior to and (b) after HTTA. Dashed line from left to right indicates *a*, *r*-sapphire substrates peak and strain-free Raman peak position of AlN respectively.

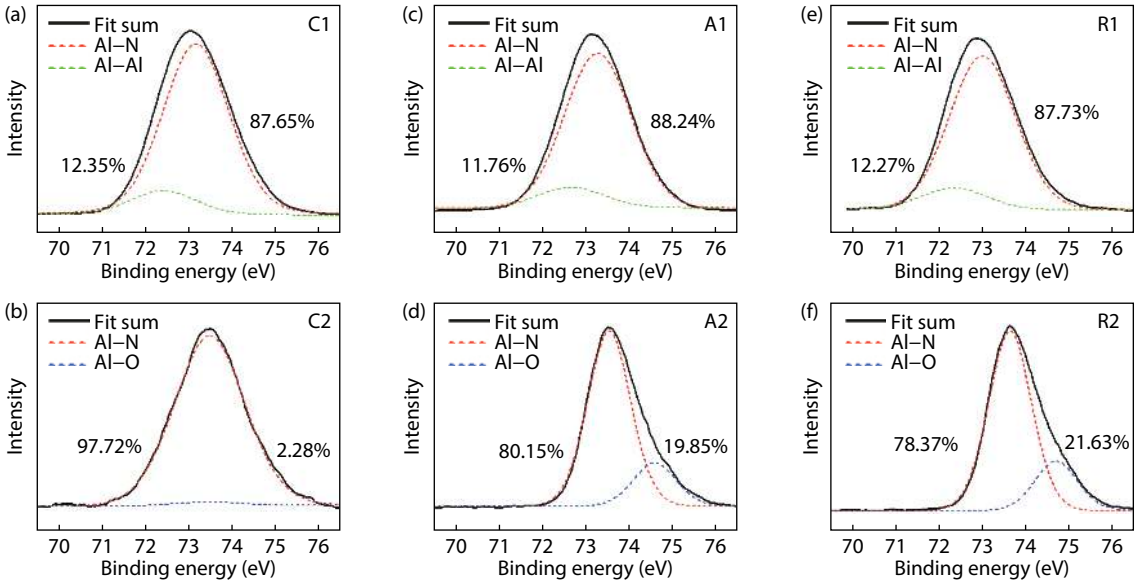

Fig. 6. (Color online) High-resolution XPS Al 2p core levels from samples grown on (a, b) *c*, (c, d) *a*, and (e, f) *r*-sapphire substrates. The core levels of Al 2p peaks are deconvoluted into Al–Al, Al–N sub-peaks before thermal annealing and Al–N, Al–O sub-peaks after thermal annealing.

Table 1. Calculated absorption edges of AlN thin films acquired by α^2 versus photon energy curve, rms roughness and the FWHM of the (002) diffraction peaks.

Sapphire orientation		Band gap (eV)	RMS (nm)	Peak FWHM (arcsec)
c-plane	C1	6.107	1.66	252
	C2	6.114	2.03	68
a-plane	A1	6.109	2.86	2494
	A2	6.126	0.717	151
r-plane	R1	6.069	5.15	–
	R2	6.081	6.11	–

the (002) diffraction peaks are summarized in Table 1. After HTTA, the bandgap of sputtered AlN on *c*-sapphire increased from 6.107 to 6.114 eV, approaching its theoretical value[35]. AlN deposited on *a* and *r*-plane sapphire substrates also follow the same trend after annealing. The enhanced bandgap of AlN after HTTA is a clear sign of reduced point defect such as V_N or V_N–oxygen complex as previously reported by Uedono *et al.*[31]. It is worth noting that compared to other defects, vacancies are supposed to have low enough formation energies in AlN thin films, which are detrimental to electronic and optical properties of the devices[29]. Our results unambiguously demonstrated that HTTA not only improved the structural property by dislocation annihilation, but also enhanced the UV transparency of AlN as a result of point defect reduction[36], laying solid foundations for the application of AlN in optoelectronic and electronic devices.

In order to identity the crystallinities and estimate the strain states in the AlN thin films deposited on various sapphire substrates, Raman spectroscopy was performed. Fig. 5 shows the Raman spectra of AlN thin films before and after HTTA. Prior to HTTA, weak E_2(high) AlN peak located at around 656 cm^{-1} is identified on C1, while the peaks are merged into the sapphire substrate peak for A1 and R1, suggesting the poor crystalline quality of AlN thin films before annealing, corroborates with the XRD characterization as revealed by Figs. 1 and 2. However, after HTTA, much stronger E_2(high) Raman modes are identified at 661 cm^{-1}, which is distinctly different to that of the *a*- and *r*-sapphire peak located at around 642 cm^{-1}. Strong compressive strains are achieved if the position of strain-free AlN at 656 cm^{-1} is considered, which is represented by the vertical dashed line[37, 38]. The large compressive strain inside the HTTA AlN might be attributed to the coalescence of the columnar domains, and all three samples exhibit the same peak position regardless of sap-

phire orientation[32]. This observation suggests that for magnetron sputtering, HTTA treatment instead of sapphire orientation plays a more significant role in determining the vibrational mode of the AlN.

To investigate the change of surface stoichiometry of sputtered AlN prior and after HTTA, high-resolution XPS spectra of the Al 2p core levels were collected, and the spectra are shown in Fig. 6. The core levels of Al 2p peak should be divided into three Gaussian-Lorentzian sub-peaks, which can be assigned to metallic aluminum, aluminum nitride and aluminum oxide from low-to-high binding energies, respectively[1]. As evident in Figs. 1(a), 1(c), and 1(e), the existence of Al-N bonds demonstrates the successful formation of AlN on sapphire for all three types of substrates. In addition, a small amount of Al–Al bonds is observed, locating at the lower binding energy, which is possibly due to the formation of wrong bonds in the crystal under magnetron sputtering. After HTTA, Al–Al wrong bonds were eliminated due to much-reduced dislocations, leading to the improvement of crystalline quality. The small amount of Al–O bond for samples after HTTA is a consequence of surface oxide formed on top of the surface as a result of trace amount of oxygen impurities inside the chamber. Finally, note that Al–N peak reveals a slight shift towards higher binding energy after HTTA. It was reported that the lower binding energy of Al 2p core level can be ascribed to lower oxidation state such as Al^{+}, Al^{2+} relative to the Al^{3+} state[39]. This agrees well with the high density of point defects including V_N in the as-deposited AlN thin film. After HTTA, the amorphous character of the AlN thin films is greatly reduced, leading to higher oxidation state of Al, and consequently higher binding energy of Al 2p peak.

4. Conclusion

In summary, high-temperature thermal annealing treatments on sputtered AlN films on *c*-, *a*- and *r*-sapphire substrates were performed. A comprehensive investigation on the structural, optical, and surface composition properties of the sputtered AlN was provided. Crystalline qualities of the AlN thin films were greatly improved after HTTA due to the annihilation of dislocations and point defects. The FWHM of the (0002) RC peak as narrow as 68 arcsec was achieved for AlN deposited on *c*-sapphire after HTTA. The bandgap of the AlN thin films increase after HTTA, demonstrating the enhanced UV transparency of AlN due to reduction of point defect. A reduction of Al–Al bonds on the surface and Al–N bonds shifting to higher binding energy after HTTA were also revealed, suggesting an increased oxidation state of Al. The improvement of structural and optical performances of sputtered AlN illustrates the great advantage of HTTA in the realization of high-quality AlN on *c*, *a* and *r*-plane sapphire substrates, providing a promising path towards the realization of high-performance AlN-based optoelectronic and electronic devices.

Acknowledgements

This work was supported by the Youth Innovation Promotion Association of the Chinese Academy of Sciences (2020298); National Key Scientific Instrument and Equipment Development Projects of China (YJKYYQ20190074); National Natural Science Foundation of China (61974149); Primary Research and Development Plan of Zhejiang Province (2020C01145); and the Natural Science Foundation of Zhejiang Province (LQ21F040004).

References

[1] Taniyasu Y, Kasu M, Makimoto T. An aluminium nitride light-emitting diode with a wavelength of 210 nanometres. Nature, 2006, 441, 325

[2] Hartmann C, Wollweber J, Dittmar A, et al. Preparation of bulk AlN seeds by spontaneous nucleation of freestanding crystals. Jpn J Appl Phys, 2013, 52, 08JA06

[3] Nagahama S I, Iwasa N, Senoh M, et al. High-power and long-lifetime InGaN multi-quantum-well laser diodes grown on low-dislocation-density GaN substrates. Jpn J Appl Phys, 2000, 39, L647

[4] Asif Khan M, Shatalov M, Maruska H P, et al. III–nitride UV devices. Jpn J Appl Phys, 2005, 44, 7191

[5] Hirayama H, Noguchi N, Fujikawa S, et al. 222–282 nm AlGaN and InAlGaN based deep-UV LEDs fabricated on high-quality AlN template. Proc SPIE 7216, Gallium Nitride Materials and Devices IV, 2009, 7216, 721621

[6] Xu H Q, Jiang J A, Chen L, et al. Direct demonstration of carrier distribution and recombination within step-bunched UV-LEDs. Photon Res, 2021, 9, 764

[7] Sun H D, Mitra S, Subedi R C, et al. Unambiguously enhanced ultraviolet luminescence of AlGaN wavy quantum well structures grown on large misoriented sapphire substrate. Adv Funct Mater, 2019, 29, 1905445

[8] Kneissl M, Seong T Y, Han J, et al. The emergence and prospects of deep-ultraviolet light-emitting diode technologies. Nat Photonics, 2019, 13, 233

[9] Xu H, Long H, Jiang J, et al. Strain modulated nanostructure patterned AlGaN-based deep ultraviolet multiple-quantum-wells for polarization control and light extraction efficiency enhancement. Nanotechnology, 2019, 30, 435202

[10] Fu H Q, Baranowski I, Huang X Q, et al. Demonstration of AlN Schottky barrier diodes with blocking voltage over 1 kV. IEEE Electron Device Lett, 2017, 38, 1286

[11] Damjanovic D. Materials for high temperature piezoelectric transducers. Curr Opin Solid State Mater Sci, 1998, 3, 469

[12] Iriarte G F. Influence of the magnetron on the growth of aluminum nitride thin films deposited by reactive sputtering. J Vac Sci Technol A, 2010, 28, 193

[13] Miyake H, Lin C H, Tokoro K, et al. Preparation of high-quality AlN on sapphire by high-temperature face-to-face annealing. J Cryst Growth, 2016, 456, 155

[14] Guo J, Wang H Y, Meng F P, et al. Tuning the H/E* ratio and E* of AlN coatings by copper addition. Surf Coat Technol, 2013, 228, 68

[15] Ben J W, Sun X J, Jia Y P, et al. Defect evolution in AlN templates on PVD-AlN/sapphire substrates by thermal annealing. CrystEngComm, 2018, 20, 4623

[16] Hagedorn S, Walde S, Mogilatenko A, et al. Stabilization of sputtered AlN/sapphire templates during high temperature annealing. J Cryst Growth, 2019, 512, 142

[17] Chen L, Lin W, Chen H Y, et al. Annihilation and regeneration of defects in $(11\bar{2}2)$ semipolar AlN via high-temperature annealing and MOVPE regrowth. Cryst Growth Des, 2021, 21, 2911

[18] Xiao S Y, Suzuki R, Miyake H, et al. Improvement mechanism of sputtered AlN films by high-temperature annealing. J Cryst Growth, 2018, 502, 41

[19] Huang C Y, Wu P Y, Chang K S, et al. High-quality and highly-transparent AlN template on annealed sputter-deposited AlN buffer layer for deep ultra-violet light-emitting diodes. AIP Adv, 2017, 7, 055110

[20] Guo W, Mitra S, Jiang J, et al. Three-dimensional band diagram in lateral polarity junction III-nitride heterostructures. Optica, 2019, 6, 1058

[21] Yan L, Zhang Y T, Han X, et al. Polarization-induced hole doping in N-polar III-nitride LED grown by metalorganic chemical vapor deposition. Appl Phys Lett, 2018, 112, 182104

[22] Meng F P, Wang B, Ge F F, et al. Microstructure and mechanical properties of Ni-alloyed SiC coatings. Surf Coat Technol, 2012, 213, 77
[23] Huang F, Ge F F, Zhu P, et al. Superhard V-Si-N coatings (>50GPa) with the cell-like nanostructure prepared by magnetron sputtering. Surf Coat Technol, 2013, 232, 600
[24] Jose F, Ramaseshan R, Dash S, et al. Response of magnetron sputtered AlN films to controlled atmosphere annealing. J Phys D, 2010, 43, 075304
[25] Iriarte G F, Reyes D F, González D, et al. Influence of substrate crystallography on the room temperature synthesis of AlN thin films by reactive sputtering. Appl Surf Sci, 2011, 257, 9306
[26] Ban K, Yamamoto J I, Takeda K, et al. Internal quantum efficiency of whole-composition-range AlGaN multiquantum wells. Appl Phys Express, 2011, 4, 052101
[27] Demir I, Li H, Robin Y, et al. Sandwich method to grow high quality AlN by MOCVD. J Phys D, 2018, 51, 085104
[28] Yoshikawa A, Nagatomi T, Morishita T, et al. High-quality AlN film grown on a nanosized concave-convex surface sapphire substrate by metalorganic vapor phase epitaxy. Appl Phys Lett, 2017, 111, 162102
[29] Ben J W, Shi Z M, Zang H, et al. The formation mechanism of voids in physical vapor deposited AlN epilayer during high temperature annealing. Appl Phys Lett, 2020, 116, 251601
[30] Moram M A, Johnston C F, Hollander J L, et al. Understanding X-ray diffraction of nonpolar gallium nitride films. J Appl Phys, 2009, 105, 113501
[31] Uedono A, Shojiki K, Uesugi K, et al. Annealing behaviors of vacancy-type defects in AlN deposited by radio-frequency sputtering and metalorganic vapor phase epitaxy studied using monoenergetic positron beams. J Appl Phys, 2020, 128, 085704
[32] Uesugi K, Hayashi Y, Shojiki K, et al. Reduction of threading dislocation density and suppression of cracking in sputter-deposited AlN templates annealed at high temperatures. Appl Phys Express, 2019, 12, 065501
[33] Gaddy B E, Bryan Z, Bryan I, et al. Vacancy compensation and related donor-acceptor pair recombination in bulk AlN. Appl Phys Lett, 2013, 103, 161901
[34] Venkatachalam S, Mangalaraj D, Narayandass S K, et al. Structure, optical and electrical properties of ZnSe thin films. Phys B, 2005, 358, 27
[35] Silveira E, Freitas J A, Schujman S B, et al. AlN bandgap temperature dependence from its optical properties. J Cryst Growth, 2008, 310, 4007
[36] Alden D, Harris J S, Bryan Z, et al. Point-defect nature of the ultraviolet absorption band in AlN. Phys Rev Appl, 2018, 9, 054036
[37] Chen S, Zhang X, Wang S C, et al. High quality non-polar a-plane AlN template grown on semi-polar r-plane sapphire substrate by three-step pulsed flow growth method. J Alloys Compd, 2021, 872, 159706
[38] Kirste R, Mita S, Hussey L, et al. Polarity control and growth of lateral polarity structures in AlN. Appl Phys Lett, 2013, 102, 181913
[39] Sharma N, Ilango S, Dash S, et al. X-ray photoelectron spectroscopy studies on AlN thin films grown by ion beam sputtering in reactive assistance of N^+/N^{2+} ions: Substrate temperature induced compositional variations. Thin Solid Films, 2017, 636, 626

Xianchun Peng received a BS degree from Nanchang Hangkong University, Nanchang, China. He is currently pursuing the master's degree in Ningbo Institute of Materials Technology and Engineering, the Chinese Academy of Sciences, in collaboration with Faculty of Materials Science and Chemical Engineering, Ningbo University, China. His current research interests are III nitride-based optoelectronic devices.

Jie Sun is currently a lab technician at Ningbo Institute of Materials Technology and Engineering (NIMTE), the Chinese Academy of Sciences. She received her master's degree from Zhejiang University of Technology, China, in 2014. Her research interests are crystal structure of inorganic materials and X-ray diffraction theory and application.

Wei Guo received his PhD from North Carolina State University, US. He then joined Applied Materials Inc. as a process engineer. He is currently an Associate Professor in Ningbo Institute of Materials Technology and Engineering, the Chinese Academy of Sciences. His research interests focus on III-nitride based wide bandgap materials, optoelectronic and electronic device.

Fanping Meng received his PhD in Materials Science and Engineering from Ningbo Institute of Materials Technology and Engineering (NIMTE), China. He is currently a Research Associate of NIMTE. His current research interests include sputter deposition of nitrides, oxides, and high-entropy alloys.

Jichun Ye received his PhD from University of California Davis. He is the deputy director of the Institute of New Energy Technology under the Ningbo Institute of Materials Technology and Engineering, Chinese Academy of Sciences, and group PI. His main research areas include the development of solar cells, UV light-emitting diodes and other optoelectronic devices. He has published more than 150 journal articles and issued more than 50 Chinese patents.